J Fluoresc
DOI 10.1007/s10895-016-1930-0

ORIGINAL ARTICLE

Synthesis, Optical Investigation and Biological Properties of Europium(III) Complexes with 2-(4-Chlorophenyl) -1-(2-Hydroxy-4-Methoxyphenyl)Ethan-1-one and Ancillary Ligands

Poonam Nandal[1] · S. P. Khatkar[1] · Rajesh Kumar[2] · Avni Khatkar[2] · V. B. Taxak[1]

Received: 14 May 2016 / Accepted: 7 September 2016

Abstract Synthesis and photoluminescence behaviour of six novel europium complexes with novel β-hydroxyketone ligand, 2-(4-chlorophenyl)-1-(2-hydroxy-4-methoxyphenyl)ethan-1-one (CHME) and 2,2′-bipyridine (bipy) or neocuproine (neo) or 1,10-phenanthroline (phen) or 5,6-dimethyl-1,10-phenanthroline (dmphen) or bathophenanthroline (bathophen) were reported in solid state. The free ligand CHME and europium complexes, $Eu(CHME)_3.2H_2O$ [1] $Eu(CHME)_3.bipy$ [2], $Eu(CHME)_3.neo$ [3], $Eu(CHME)_3.phen$ [4], $Eu(CHME)_3.dmphen$ [5] and $Eu(CHME)_3.bathophen$ [6]were characterized by elemental analysis, FT-IR and ^{1}H-NMR. The photoluminescence emission spectra exhibited four characteristic peaks arising from the $^5D_0 \rightarrow {}^7F_J$ (J = 1–4) transitions of the europium ion in the solid state on monitoring excitation at λ_{ex} = 395 nm. The luminescence decay curves of these europium complexes possess single exponential behaviour indicating the presence of a single luminescent species and having only one site symmetry in the complexes. The luminescence quantum efficiency (η) and the experimental intensity parameters, Ω_2 and Ω_4 of europium complexes have also been calculated on the basis of emission spectra and luminescence decay curves. In addition, the antimicrobial and antioxidant activities were also studied of the investigated complexes.

✉ V. B. Taxak
v_taxak@yahoo.com

[1] Department of Chemistry, Maharshi Dayanand University, Rohtak 124001, India

[2] UIET, Maharshi Dayanand University, Rohtak 124001, India

Keywords Eu(III) complexes · Photoluminescence · Quantum efficiency · Judd-Ofelt intensity parameters · Antimicrobial activity · Antioxidant activity

Introduction

The lanthanide complexes with organic ligand have been widely studied from last few decades due to their potential applications in full color flat-panel displays [1–3], organic light emitting diodes (OLEDs) [4, 5], optical telecommunications [6–8] and medical applications [9, 10]. As a result lot of attention have been paid on the synthesis and photoluminescent investigation of novel lanthanide complexes with organic ligand possessing excellent luminescent properties [11–13]. Most of the lanthanide ions emit in entire spectroscopic region from UV (Gd^{3+}) to visible (blue, Tm^{3+}; white, Dy^{3+}; green, Tb^{3+}; orange, Sm^{3+} and red, Eu^{3+}) and NIR (Pr^{3+}, Yb^{3+}, Nd^{3+} and Er^{3+}) [14]. Among these lanthanide ions, Eu^{3+} ion has large energy gap between the lowest luminescent energy state to highest non-luminescent energy state; thus gives rise to tremendously sharp and strong emission in the visible region. The Eu^{3+} offers four characteristic emission lines at 593 nm ($^5D_0 \rightarrow {}^7F_1$), 616 nm ($^5D_0 \rightarrow {}^7F_2$), 650 nm ($^5D_0 \rightarrow {}^7F_3$) and 685 nm ($^5D_0 \rightarrow {}^7F_4$). Out of these transitions $^5D_0 \rightarrow {}^7F_2$ being intense is responsible for the bright red color of complexes. However, direct excitation of lanthanide ions is extremely difficult because trivalent lanthanide cations have low molar extinction coefficient ($\varepsilon < 1\ M^{-1}\ cm^{-1}$) due to Laporte forbidden 4f-4f electronic transitions of lanthanide ions [15–17]. To overcome this drawback, we must incorporate organic ligands having high absorption coefficient which can act as photosensitizer. The chelating organic ligand efficiently absorbs and transfer energy to trivalent lanthanide ions through "antenna effect" [18–21],

Published online: 19 September 2016

resulting in intense lanthanide ion emission. Therefore, the design of efficient ligands has become an important goal for research. It is well known that O,O- or O,N- or N,N- chelate group with extended conjugated system including β-diketones, aromatic carboxylic acids, pyridine derivatives, nuclic acids, quinoline derivatives, cryptends and several other macrocyclic ligands [22–24] have received considerable interest and have been extensively applied in the synthesis of luminescent lanthanide complexes. But little attention has been paid for the synthesis of lanthanide complexes with β-hydroxyketones. Our previous research results indicate that β-hydroxyketones have strong absorption coefficient and efficiently sensitize the luminescence of Eu^{3+}, $Tb^{3+}$and Sm^{3+}ions. Moreover nitrogen containing non charged heterocyclic ligands like 2,2′-bipyridine (bipy) or neocuproine (neo), or 1,10-phenanthroline (phen) or 5,6-dimethyl-1,10-phenanthroline (dmphen) or bathophenanthroline (bathophen) serves synergistic effect and enhance the photoluminescent intensity by transfer of the energy from ligand to central metal ion through antenna effect.

In present section focus is on the synthesis of β-hydroxyketone, 2-(4-chlorophenyl)-1-(2-hydroxy-4-methoxyphenyl)ethan-1-one (CHME). With the CHME as the main ligand and 2,2′-bipyridine (bipy) or neocuproine (neo), or 1,10-phenanthroline (phen) or 5,6-dimethyl-1,10-phenanthroline (dmphen) or bathophenanthroline (bathophen) as ancillary ligand six novel europium complexes were synthesized in order to achieve effective luminescence performance.

Experimental Details

Materials and Instrumentation

Europium nitrate hydrate [$Eu(NO_3)_3$. H2O], 2,2′-bipyridine, neocuproine, 1,10-phenanthroline, 5,6-dimethyl-1,10-phenanthroline and bathophenanthroline were purchased from Sigma-Aldrich. Resorcinol, 4-chlorobenzylcyanide, anhydrous zinc chloride, potassium carbonate, dimethyl sulphate were purchased from Hi-Media Pvt. Ltd. The reagent employed were of analytical grade and used without any further purification. Solvents were freshly distilled with standard methods. Synthesized ligand CHME was recrystalized three times with methanol before the synthesis of complexes. Microbial strains Gram-positive bacteria: *Staphylococcus aureus* (MTCC 3160), *Bacillus subtilis* (MTCC 441), and Gram-negative bacterium: *Escherichia coli* (MTCC 443) and fungal strains: *Candida albicans* (MTCC 227) *Aspergillus niger* (MTCC 281) were purchased from Institute of microbial Technology, Sector 39-A, Chandigarh, India. Nutrient broth medium, nutrient agar medium, subourand dextrose agar medium and subourand dextrose broth medium, dimethyl sulfoxide (DMSO) were purchased from Hi-Media Pvt. Ltd. 1,1-Diphenyl-2-picrylhydrazylradical (DPPH) were purchased from Sigma-Aldrich.

The europium content of the complexes was estimated by complexometric titration with EDTA using xylenol orange as an indicator. Elemental analysis (C, H and N) was performed using thermo scientific flash 2000 elemental analyzer. FT-IR spectra were obtained on Perkin Elmer spectrum 400 FT-IR spectrometer by using KBr disks in the range of 4000–400 cm^{-1}. The ^{1}H-NMR spectra were recorded on Bruker Avance II 400 spectrometer (400 MHZ) in dimethylsulfoxide solution. The ^{13}C-NMR spectra were measured on Jeol: JNM-EXCP 400; 400 MHz FT-NMR spectrometer. The excitation and emission spectra of complexes in the UV-Visible region and decay curves under time scan mode were measured on Hitachi F-7000 fluorescence spectrophotometer equipped with Xe-lamp at room temperature in solid state. The life time values of the complexes were calculated with the help of software of the spectrophotometer (FL solution for F-7000). The UV-Visible absorption spectra were measured on Shimadzu-2450 UV-Vis spectrophotometer.

Synthesis

Synthesis of Ligand 2-(4-Chlorophenyl) -1-(2-Hydroxy-4-Methoxyphenyl)Ethan-1-one (CHME)

The ligand was synthesized in two steps by using Houben-Hoesch reaction mechanism between resorcinol and 4-chlorobenzylcyanide. The first step involves the preparation of 2-(4-chlorophenyl)-1-(2,4-dihydroxyphenyl)ethan-1-one (CDHPE) and the second step involves the preparation of 2-(4-chlorophenyl)-1-(2-hydroxy-4-methoxyphenyl)ethan-1-one (CHME) which are described as follows:

Step 1. Synthesis of 2-(4-chlorophenyl)-1-(2,4-dihydroxyphenyl)ethan-1-one (CDHPE)

A mixture of resorcinol (10 g), 4-chlorobenzylcyanide (7 g) and powered anhydrous $ZnCl_2$ were added in dry ether (100 mL). The mixture was cooled at 0 °C and rapid HCl gas was passed for 5 h. After leaving over night in ice chest, the orange yellow precipitate of ketimine hydrochloride was separated by decanting ether and washed twice with dry ether (20 mL). The solid was refluxed with water (200 mL) for 1 h. On cooling 2-(4-chlorophenyl)-1-(2,4-dihydroxyphenyl)ethan-1-one (CDHPE) was separated as pale yellow needles, which were filtered and dried at 120 °C.

Step 2. Synthesis of 2-(4-chlorophenyl)-1-(2-hydroxy-4-methoxyphenyl)ethan-1-one (CHME)

A solution of CDHPE (5 g) in dry acetone (50 mL) was refluxed with dimethyl sulphate (7.3 mL) and freshly ignited potassium carbonate (25 g) for 2 h. The inorganic salt was filtered and washed with hot acetone. Acetone was distilled off from filtrate and ice cold water was added to oily residue when colorless solid separated out. Solid was filtered, washed with water and recrystalized three times with methanol to give CHME. The progress of the reaction was monitored by thin layer chromatography. CHME was obtained as white crystals with 78 % yield, m.pt. 219-220 °C. The synthetic route of ligand CHME is given in Scheme 1. The elemental analysis data for CHME ($C_{15}H_{13}O_3Cl$) was found (calc.) % C, 65.18 (65.10); H, 4.76 (4.73).

IR (KBr)cm^{-1}: 3429 (b), 3055 (m), 3022 (w), 2940 (w), 2842 (w), 1650 (s), 1633 (s), 1596 (s), 1567 (s), 1494 (s), 1439 (s), 1351 (s), 1310 (m), 1291 (s), 1229 (s), 1207 (s), 1197 (s), 1084 (s), 1028 (s), 994 (s), 822 (s), 810 (s), 777 (s), 600 (s), 581 (s). ^{1}H-NMR (400 MHz, DMSO, δ, ppm): 3.83 (s, 3H, OCH_3), 4.18 (s, 2H, CH_2), 6.42 (s, 1H, Ar-H), 6.43 (s, 1H, Ar-H), 7.24 (d, 2H, Ar-H), 7.30 (d, 2H, Ar-H), 7.57 (s, 1H, Ar-H), 12.61 (s, 1H, OH). ^{13}C-NMR (400 MHz, DMSO, δ, ppm): 201.7, 166.6, 165.5, 133.2, 131.2, 131.0, 129.9, 129.3, 112.8, 106.8, 103.2, 55.8, 40.2.

Synthesis of Complexes

Eu(CHME)$_3$. 2H$_2$O [1] In a ethanolic solution of CHME (0.82 g, 3 mmol) add an aqueous solution of $Eu(NO_3)_3$. H2O (0.33 g, 1 mmol) was added with constant stirring on magnetic stirrer. The solution was neutralized with 0.05 M NaOH solution and adjusted pH of mixture 7 8. The mixture was stirred for 3 h at 35 °C and then allowed to stand for 1 h. During stirring white precipitates appeared, which were filtered and washed with doubly distilled water and then with ethanol to remove the free ligand, after that dried in air and then in vacuum desiccators. Finally the complex was dried at 50 °C in hot air oven to obtain the complex. The obtained complex Eu(CHME)$_3$.2H$_2$O was white power with 86 % yield. The elemental analysis data for Eu(CHME)$_3$.2H$_2$O ($C_{45}H_{40}O_{11}Cl_3Eu$) was found (calc.) % C, 53.21 (53.24); H, 4.06 (3.97); Eu, 14.92 (14.97).

IR (KBr)cm^{-1}: 3447 (b), 3063 (w), 2944 (m), 2427 (w), 1706 (s), 1630 (s), 1560 (s), 1493 (m), 1422 (s), 1384 (s), 1338 (s), 1285 (m), 1223 (s), 1155 (s), 1084 (m), 1032 (s), 993 (w), 944 (w), 813 (m), 783 (m), 733 (m), 640 (m), 497 (m). ^{1}H-NMR (400 MHz, DMSO, δ, ppm): 3.47 (s, 9H, OCH_3), 4.26 (s, 6H, CH_2), 6.45 (bd, 6H, Ar-H), 7.29 (d, 6H, Ar-H), 7.91 (d, 6H, Ar-H), 8.09 (s, 3H, Ar-H). ^{13}C-NMR (400 MHz, DMSO, δ, ppm): 197.4, 166.6, 158.3, 133.2, 131.2, 131.0, 129.9, 129.3, 110.7, 106.8, 101.2, 55.8, 38.4.

Ternary Eu(III) complexes 2–6 were also prepared using same procedure as adopted in the synthesis of complex 1, taking the mixture of 3 mmol CHME, 1 mmol corresponding ancillary ligand and 1 mmol europium nitrate. The synthetic route and the structure of Eu(III) binary and ternary complexes 1–6 are given in Scheme 2.

Eu(CHME)$_3$. Bipy [2] The obtained complex was white power with 78 % yield. The elemental analysis data for Eu(CHME)$_3$.bipy ($C_{55}H_{44}O_9Cl_3N_2Eu$) was found (calc.) % C, 58.21 (58.18); H, 3.86 (3.90); N, 2.42 (2.46); Eu, 13.31 (13.38).

IR (KBr)cm^{-1}: 3084 (w), 3010 (w), 2942 (m), 2843 (m), 1706 (s), 1606 (s), 1589 (s), 1525 (s), 1493 (s), 1468 (s), 1456 (s), 1415 (s), 1384 (s), 1292 (s), 1229 (s), 1206 (s), 1154 (s), 1126 (s), 1084 (s), 1030 (m), 992 (m), 944 (m), 868 (m), 812 (s), 782 (m), 734 (s), 664 (m), 640 (m), 586 (m), 539 (w), 496 (m). ^{1}H-NMR (400 MHz, DMSO, δ, ppm): 3.80 (s, 9H, OCH_3), 4.29 (s, 6H, CH_2), 6.45 (bd, 6H, Ar-H), 7.13–7.38 (bs, 14H,12 Ar-H and 2H bipy), 8.14 (s, 3H, Ar-H), 8.59 (d,

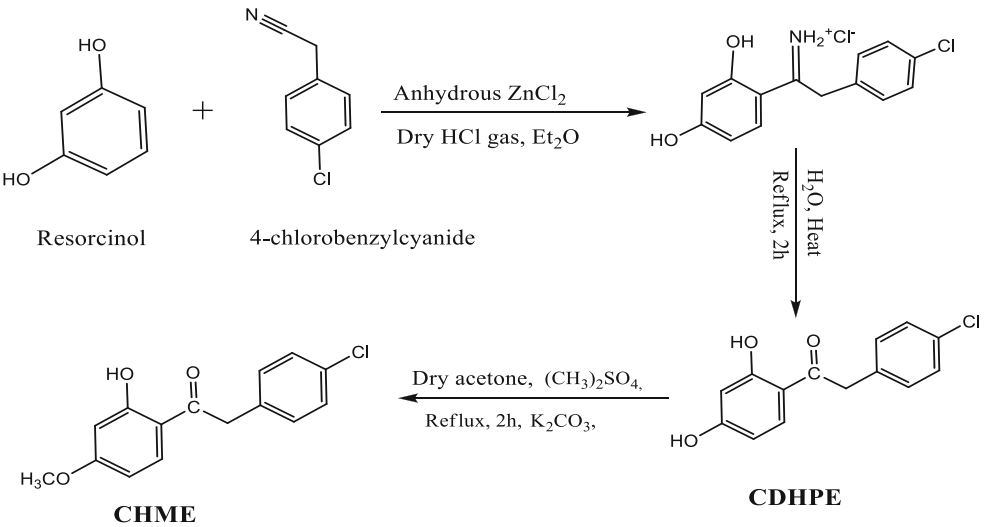

Scheme 1 The synthetic route of ligand CHME

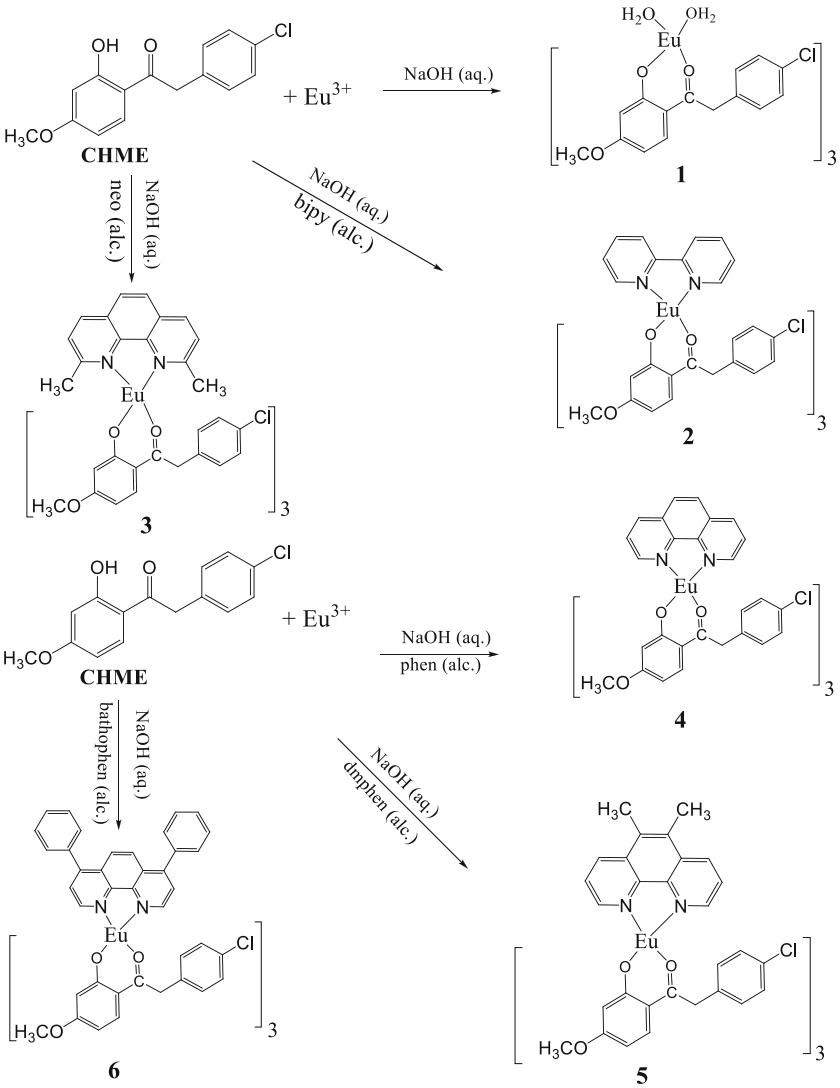

Scheme 2 The synthetic route and structure of Eu(III) binary and ternary complexes 1–6 with CHME

2H, bipy), 8.71 (d, 2H, bipy), 9.21 (d, 2H, bipy). ^{13}C-NMR (400 MHz, DMSO, δ, ppm): 195.4, 166.6, 162.2, 155.3, 148.2, 137.2, 133.2, 131.2, 131.0, 129.9, 129.3, 123.6, 121.4, 109.6, 106.8, 98.4, 55.8, 37.2.

Eu(CHME)$_3$. Neo [3] The complex Eu(CHME)$_3$.neo was obtained as white power with 81 % yield. The elemental analysis data for Eu(CHME)$_3$.neo ($C_{59}H_{50}O_9Cl_3N_2Eu$) was found (calc.) % C, 59.49 (59.58); H, 4.19 (4.23); N, 2.31 (2.35); Eu, 12.73 (12.77).

IR (KBr)cm^{-1}: 3094 (w), 2927 (w), 2495 (w), 2317 (w), 1975 (w), 1767 (w), 1607 (s), 1583 (s), 1543 (s), 1495 (s), 1384 (s), 1342 (m), 1300 (s), 1218 (s), 1191 (m), 1167 (s), 1123 (m), 1080 (s), 1030 (s), 949 (m), 812 (s), 734 (s), 689 (m), 640 (m), 620 (m), 549 (w), 427 (w). ^{1}H-NMR (400 MHz, DMSO, δ, ppm): 2.53 (s, 6H, neoCH_3), 3.39 (s, 9H, OCH_3), 4.21 (s, 6H, CH_2), 6.41–6.56 (bd, 6H, Ar-H), 7.30–7.76 (bs, 12H, Ar-H), 7.88 (d, 2H, neo) 8.30 (s, 3H, Ar-H), 8.61 (d, 2H, neo), 9.15 (d, 2H, neo). ^{13}C-NMR (400 MHz, DMSO, δ, ppm): 198.3, 166.6, 162.2, 158.2, 144.3, 135.6, 133.2, 131.2, 131.0, 129.9, 129.3, 128.1, 126.8, 124.2, 110.2, 106.8, 99.8, 55.8, 38.4, 25.2.

Eu(CHME)$_3$. Phen [4] The obtained complex was white power with 92 % yield. The elemental analysis data for Eu(CHME)$_3$.phen ($C_{57}H_{44}O_9Cl_3N_2Eu$) was found (calc.) % C, 59.13 (59.05); H, 3.79 (3.82); N, 2.44 (2.41); Eu, 13.08 (13.10).

IR (KBr)cm^{-1}: 3063 (w), 2925 (w), 2493 (w), 2298 (w), 1765 (w), 1626 (m), 1592 (m), 1577 (m), 1474 (s), 1424 (s), 1384 (s), 1344 (m), 1306 (s), 1221 (s), 1141 (m), 1103 (s), 1031 (s), 991 (w), 863 (m), 842 (s), 814 (m), 765 (m), 736 (m), 725 (s), 638 (m), 553 (w), 511 (w), 475 (w). ^{1}H-NMR (400 MHz, DMSO, δ, ppm): 3.84 (s, 9H, OCH_3), 4.19 (s, 6H, CH_2), 6.43 (d, 6H, Ar-H), 7.19 (d, 6H, Ar-H), 7.21 (d, 6H, Ar-H) 7.26 (d, 2H, phen), 7.32 (d, 2H, phen), 7.70 (d, 2H, phen), 7.73 (d, 2H, phen), 8.30 (s, 3H, Ar-H). ^{13}C-NMR (400 MHz, DMSO, δ, ppm):

195.8, 166.6, 158.4, 148.8, 146.2, 136.4, 133.2, 131.2, 131.0, 129.9, 129.3, 129.2, 127.6, 121.5, 110.5, 106.8, 101.9, 55.8, 38.4.

Eu(CHME)$_3$. Dmphen [5] Eu(CHME)$_3$.dmphen was obtained as white power with 89 % yield. The elemental analysis data for Eu(CHME)$_3$.dmphen ($C_{59}H_{50}O_9Cl_3N_2Eu$) was found (calc.) % C, 59.61 (59.58); H, 4.21 (4.23); N, 2.38 (2.35); Eu, 12.79 (12.77).

IR (KBr)cm^{-1}: 3095 (w), 2927 (w), 2495 (w), 2318 (w), 1976 (w), 1767 (w), 1608 (s), 1584 (s), 1542 (s), 1484 (s), 1433 (s), 1384 (s), 1343 (m), 1300 (s), 1222 (w), 1191 (m), 1168 (s), 1124 (m), 1080 (s), 1031 (s), 950 (m), 812 (s), 735 (s), 689 (m), 641 (m), 621 (m), 550 (w), 427 (w). ^{1}H-NMR (400 MHz, DMSO, δ, ppm): 2.53 (s, 6H, dmphenCH_3), 3.38 (s, 9H, OCH_3), 4.19 (s, 6H, CH_2), 6.41–6.56 (b, 6H, Ar-H), 7.24–7.78 (b, 12H, Ar-H), 7.92 (d, 2H, dmphen), 8.11 (s, 3H, Ar-H), 8.51 (d, 2H, dmphen), 9.20 (d, 2H, dmphen). ^{13}C-NMR (400 MHz, DMSO, δ, ppm): 195.6, 166.6, 158.2, 148.2, 143.9, 134.0, 133.2, 131.2, 131.0, 129.9, 129.7, 129.3, 129.1, 121.1, 110.6, 106.8, 101.6, 55.8, 38.2, 21.1.

Eu(CHME)$_3$. Bathophen [6] This complex was obtained as white power with 90 % yield. The elemental analysis data for Eu(CHME)$_3$.bathophen ($C_{69}H_{55}O_9Cl_3N_2Eu$) was found (calc.) % C, 63.09 (63.04); H, 4.23 (4.21); N, 2.17 (2.13); Eu, 11.52 (11.56).

IR (KBr)cm^{-1}: 3010 (m), 2941 (m), 2845 (m), 1706 (s), 1605 (s), 1589 (m), 1522 (m), 1492 (s), 1468 (s), 1414 (s), 1384 (s), 1340 (m), 1224 (s), 1206 (s), 1183 (m), 1154 (s), 1127 (s), 1085 (s), 1032 (m), 1015 (m), 993 (m), 834 (s), 813 (m), 740 (m), 703 (m), 640 (w), 574 (w), 544 (w), 496 (w). ^{1}H-NMR (400 MHz, DMSO, δ, ppm): 3.83 (s, 9H, OCH_3), 4.19 (s, 6H, CH_2), 6.45–6.58 (d, 6H, Ar-H), 7.53 (b, 12H, Ar-H), 7.82–7.96 (b, 14H, bathophen), 8.12 (s, 3H, Ar-H), 9.23 (d, 2H, bathophen). ^{13}C-NMR (400 MHz, DMSO, δ, ppm): 197.2, 166.6, 158.4, 151.4, 149.4, 145.1, 140.3, 133.2, 131.2, 131.0, 129.9, 129.3, 129.2, 127.3, 123.1, 120.3, 111.3, 109.8, 106.8, 101.8, 55.8, 38.3.

Biological Evaluation of Synthesized Complexes

Antimicrobial Activity

Antibacterial activity of newly synthesized 2-(4-chlorophenyl)-1-(2-hydroxy-4-methoxyphenyl)ethan-1-one (CHME) and its corresponding six new Eu(III) complexes were performed against Gram-positive bacteria: *Staphylococcus aureus* (MTCC 3160), *Bacillus subtilis* (MTCC 441), and Gram-negative bacterium: *Escherichia coli* (MTCC 443) and fungal strains: *Candida albicans* (MTCC 227) and *Aspergillus niger* (MTCC 281) using tube dilution method. Ciprofloxacin (antibacterial) and fluconazole (antifungal) were the standard drug as references. The standard drug, CHME and the Eu(III) complexes were dissolved in DMSO to prepare a stock solution of the concentration of 100 μg/mL. Dilutions of test samples and standard drugs were prepared in double strength nutrient broth I.P. (bacteria) or sabouraud dextrose broth I.P. (fungi). The test samples were incubated at and 7 days at respectively.

MIC values were evaluated for four different concentrations (50, 25, 12.5 and 6.25) for each test samples and the standard drugs. These different concentrations were obtained by tube dilution in autoclaved nutrient broth in assay tubes. 0.1 mL of normal saline suspension of strains (1.0×10^5 c.f.u./mL of microorganism) was added to each test tubes. The test samples were incubated at 37 °C for 24 h (bacteria), at 37 °C for 48 h (*Candida albicans)* and at 25 °C for 7 days (*Aspergillus niger)*. The results were recorded in terms of MIC (the lowest concentration of test substance which inhibited the growth of microorganisms) by observing turbidity in assay tubes.

In Vitro Antioxidant Activity

Free radical scavenging activity of ligand 2-(4-chlorophenyl)-1-(2-hydroxy-4-methoxyphenyl)ethan-1-one (CHME) and its corresponding Eu(III) complexes against nitrogen centered most familiarly used stable free radical 2, 2-diphenyl-2-picrylhydrazyl hydrate (DPPH), was most employed used to determine antioxidant activity spectrophotometrically based on the fact that odd electron present in the DPPH free radical reacts with antioxidant complex, its deep violet colour in methanol bleaches to yellow, gives a strong absorbance, which maximises at λ = 517 nm. Stock solution of various concentrations (25, 50, 75, and 100) μg/ml of the complexes dissolved in methanol was added to 5 ml of a 0.004 % methanol solution of DPPH. The mixtures were vigorously shaken and allowed to stand for 30 min in the dark at room temperature for incubation. Tests were carried out in triplicate. By using UV-Visible spectrophotometer, absorbance value was measured at λ = 517 nm. The DPPH scavenging activity was expressed as IC_{50}, whose concentration is sufficient to obtain 50 % of maximum scavenging activity. Standard curve was plotted for different concentration of ascorbic acid and complexes. Scavenging of DPPH free radical was calculated as:

$$\text{DPPH scavenging activity}(\%) = 100\frac{(A_0\text{-}A_s)}{A_0}$$

Where, A_0 is the absorbance of the control reaction (containing all reagents except test complexes) and A_s is the absorbance of the test complexes. The observed results were compared with the activity of ascorbic acid, which was used as the standard.

Results And Discussion

Elemental Analysis and Solubility

The elemental analysis data for the synthesized ligand CHME and its corresponding Eu(III) binary and ternary complexes 1–6 are tabulated in Table 1. The results revealed that the ligand CHME and its corresponding Eu(III) complexes were successfully synthesized. The ternary complexes 2–6 were found in the ratio 1:3:1 i.e. europium metal to ligand CHME to ancillary ligand. The complexes were white powder, stable under atmospheric condition and soluble in DMSO, chloroform, dichloromethane, acetone, methanol and ethanol but insoluble in benzene and hexane.

NMR and IR Spectra

The assignments of ^{1}H-NMR and ^{13}C-NMR spectra of Eu(III) complexes disclose some afferent changes as compared to the free ligand CHME due to paramagnetism of metal ion. The ^{1}H-NMR spectrum of free ligand CHME exhibits a singlet of phenolic OH proton at δ 12.61 ppm which was not observed in the complexes, indicating that the ligand was involved in the coordination with the Eu^{3+} through the phenolic oxygen atom of CHME. In the ^{13}C-NMR spectra, the carbon values in free ligand appeared at 201.7 (C = O), 165.5 (C–O), 112.8 (=C–), 103.3 (−C=) and 40.2 (−CH_2–) which shifted upfield in the corresponding complexes 1–6 (198.3–195.4 (C = O), 162.2–158.2 (C–O), 110.7–109.6 (=C–), 109.6–98.4 (=C–), 38.4–37.2 (−CH_2).

The formation of complexes 1–6 were also observed by FT-IR absorption spectra. The FT-IR absorption spectra of complexes 1–6 exhibited some observable changes in comparison with the free ligand CHME which are summarized in Table 2 along with their characteristic assignments. In the FT-IR spectra of free ligand CHME a broad absorption band appeared at 3429 cm^{-1} due to ν(O-H) which was red shifted 18 cm^{-1} in case of binary complex 1,while disappeared in the ternary complexes 2–6 implying that the ligand CHME was coordinated with the metal ion in a mode of deprotonated phenolic OH group. The strong absorption band in the region 1630–1605 cm^{-1} due to C = O stretching vibrations [25, 26] were red shifted 3–28 cm^{-1} with respect to those of free ligand CHME due to extended conjugation present in the complexes, confirming the coordination of the carbonyl oxygen atom with the metal ion. A new absorption band in the complexes 2–6 appeared at 1592–1583 cm^{-1} assigned to C = N stretching vibration of ancillary ligand [27], indicated that nitrogen atom of ancillary ligands can also participate in the coordination. In the complexes 2–6, weak absorption band at 539 cm^{-1} and 497–427 cm^{-1} shows the presence of Eu-N and Eu-O stretching vibrations [28, 29] respectively, which was not observed in the spectra of binary complex 1 and ligand, this indicated that in the ternary complexes nitrogen atom of the ancillary ligand also coordinated with the Eu^{3+} ion. All these changes in the spectra confirmed that Eu^{3+} ion coordinated with the ligand through phenolic and carbonyl oxygen atom of the ligand CHME and nitrogen atoms of respective ancillary ligand, while in case of complex 1, Eu^{3+} ion coordinated with the phenolic and carbonyl oxygen atom of the ligand and two oxygen atoms of water molecules. The elemental analysis, ^{1}H-NMR, ^{13}C-NMR spectra and FT-IR spectra of ligand and its Eu(III) complexes 1–6, all were in well agreement with Scheme 2.

Photoluminescent Properties

Figure 1 depicts the photoluminescence excitation spectra of complexes 1–6 in solid state at room temperature on monitoring emission at λ_{em} = 617 nm. The inset depicts the broad excitation band of ligand CHME at about 382 nm with low intensity due to π-π* transition in the ligand. The excitation band in the complexes 1–6 stay in a wide range 300–425 nm, centred at 395 nm with remarkable increase in intensity. As a comparison, the complex $Eu(CHME)_3$.bathophen shows higher intensity due to the formation of a bigger π-conjugation present in the complex.

Figure 2 shows the photoluminescence emission spectra of complexes 1–6 on monitoring excitation at λ_{ex} = 395 nm. The emission spectra of all the complexes exhibited four

Table 1 Elemental analysis data for ligand CHME and its corresponding Eu(III) complexes 1–6

Complexes	C (%) found (calc.)	H (%) found (calc.)	N (%) found (calc.)	Eu (%) found (calc.)
CHME	65.18 (65.10)	4.76 (4.73)	—	—
1	53.21 (53.24)	4.06 (3.97)	—	14.92 (14.97)
2	58.21 (58.18)	3.86 (3.90)	2.42 (2.46)	13.31 (13.38)
3	59.49 (59.58)	4.19 (4.23)	2.31 (2.35)	12.73 (12.77)
4	59.13 (59.05)	3.79 (3.82)	2.44 (2.41)	13.08 (13.10)
5	59.61 (59.58)	4.21 (4.23)	2.38 (2.35)	12.79 (12.77)
6	63.09 (63.04)	4.23 (4.21)	2.17 (2.13)	11.52 (11.56)

Table 2 The characteristic IR bands (cm^{-1}) of the free ligand CHME and its corresponding Eu(III) complexes 1–6

Complexes	ν(O-H)	ν(C = O)	ν(C = N)	ν(C = C)	ν(Ph-O)	ν(Eu-N)	ν(Eu-O)
CHME	3429 (b)	1633 (s)	—	1567 (s)	1229 (s)	—	—
1	3447 (b)	1630 (s)	—	1560 (s)	1223 (s)	—	497 (m)
2	—	1606 (s)	1589 (s)	1525 (s)	1292 (s)	539 (w)	496 (m)
3	—	1607 (s)	1583 (s)	1543 (s)	1218 (s)	549 (m)	427 (m)
4	—	1626 (m)	1592 (m)	1577 (s)	1221 (s)	511 (m)	475 (m)
5	—	1608 (s)	1584 (s)	1542 (s)	1222 (s)	550 (w)	427 (m)
6	—	1605 (s)	1589 (m)	1522 (m)	1224 (s)	544 (m)	496 (m)

b = broad, s = strong, m = medium, w = weak

characteristic peaks for the $^5D_0 \rightarrow {}^7F_J$ (J = 1–4) transitions assigned to $^5D_0 \rightarrow {}^7F_1$ (593 nm), $^5D_0 \rightarrow {}^7F_2$ (617 nm), $^5D_0 \rightarrow {}^7F_3$ (650 nm) and $^5D_0 \rightarrow {}^7F_4$ (684 nm). The $^5D_0 \rightarrow {}^7F_2$ (617 nm) transition is an electric dipole-allowed transition and is extremely sensitive to site symmetry of the Eu^{3+} ion [30, 31] whereas the magnetic dipole transition $^5D_0 \rightarrow {}^7F_1$ (593 nm) is insensitive to site symmetry [32]. The $^5D_0 \rightarrow {}^7F_2$ transition is approximately 3–6 times stronger than $^5D_0 \rightarrow {}^7F_1$ transition, indicating a highly polarisable chemical environment around the central Eu^{3+} ion responsible for the bright red color of these complexes. Moreover, after the introduction of ancillary ligands, the emission intensity of complexes 2–6 was greatly enhanced as compared to the binary complex [33], due to the synergetic effect of N,N-donor ancillary ligands which causes an efficient energy transfer from the ligands to central Eu^{3+} ion [34]. The complex $Eu(CHME)_3$.bathophen showed prominent photoluminescent intensity may be due to extended conjugation of π electrons in the presence of ancillary ligand bathophenanthroline.

Luminescence Lifetime and Quantum Efficiency

PL decay curves for complexes 1–6 corresponding to $^5D_0 \rightarrow {}^7F_2$ transition (616 nm) under excitation at 395 nm in solid state are depicted in Fig. 3. The luminescence decay time is affected by luminescent centres, energy transfer, defects and impurities present in the complexes. The time resolved $^5D_0 \rightarrow {}^7F_2$ transition of all synthesized complexes obey single exponential curve which can be calculated by applying the eq. $I = I_o\, exp.\ (-t/\tau)$, where τ is the radiative decay time I and I_o are the luminescence intensities at time t and 0, respectively. The luminescence decay curves of these europium complexes possess single exponential behaviour indicating the presence of a single luminescent species and having only one site symmetry in the complexes 1–6 [35–37]. The lifetime values calculated for complexes 1–6 were found to be 0.493 ms [1], 0.632 (2), 0.842 (3), 0.867 (4), 0.896 (5) and 0.912 ms [6] respectively as tabulated in Table 3. The relative shorter lifetime value observed for complex $Eu(CHME)_3.2H_2O$ [1] may be due to the dominant nonradiative decay pathway because of the presence of water molecules in this complex, as reported in many binary europium complexes [38]. The much longer lifetime value for complex 6 has been observed as compared to complexes 1–5, which may be due to extended conjugation present in the complex 6.

The *Commission Internationale de Eclairage* (CIE) coordinate of the photoluminescence spectra of these europium complexes 1–6 has been analyzed with the help

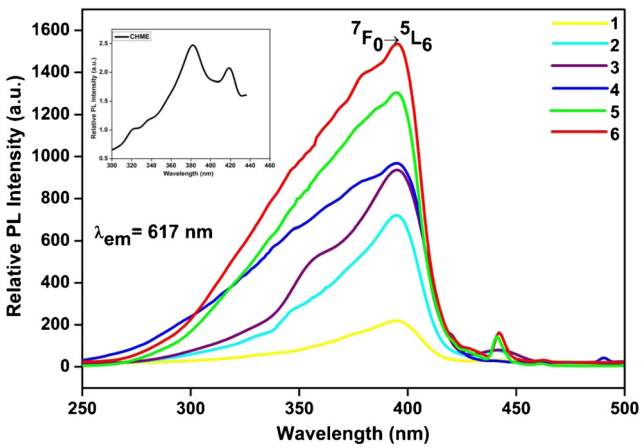

Fig. 1 Photoluminescence excitation spectra of complexes 1–6, monitored at λ_{em} = 617 nm in solid state at room temperature and inset shows the excitation spectrum of ligand CHME

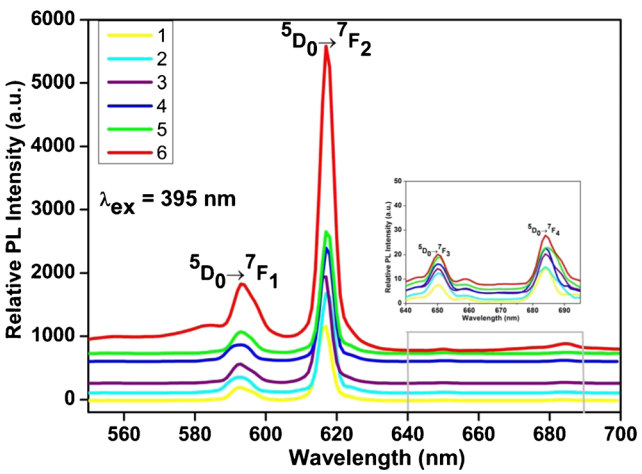

Fig. 2 Photoluminescence emission spectra of complexes 1–6 in solid state at room temperature, monitored at λ_{ex} = 395 nm

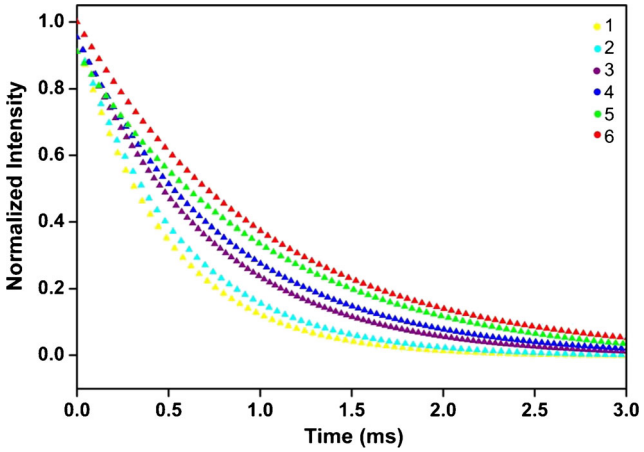

Fig. 3 Luminescence decay curves of the $^5D_0 \rightarrow {}^7F_2$ transition for Eu(III) complexes 1–6 in solid state at room temperature, monitored at λ_{ex} = 395 nm

of CIE chromaticity coordinate diagram. The CIE color coordinates (*x*, *y*) of the complexes 1–6 are located at (0.5925, 0.4063), (0.6237, 0.3643), (0.6016, 0.3715), (0.6348, 0.3425), (0.6551, 0.3444) and (0.6570, 0.3235) as shown in Fig. 4, which fall in deep red spectral region. These Eu(III) complexes might exhibit promising applications in display devices.

The emission spectra and lifetimes values of the complexes have been exploited for the determination of the luminescent quantum efficiency (η) using the equation (1) [39]:

$$\eta = \frac{A_{rad}}{A_{rad}+A_{nrad}} \tag{1}$$

Where A_{rad} is the radiative transition rate and A_{nrad} is the non radiative transition rate. The obtained radiative decay rates A_{rad}, non radiative decay rates A_{nrad} and luminescence quantum efficiency (η) of these europium complexes 1–6 are tabulated in Table 3 which were determined in solid state at room temperature. The A_{rad} can be calculated by summing over the radiative rates A_{0J} for each $^5D_0 \rightarrow {}^7F_J$ transition. The transition $^5D_0 \rightarrow {}^7F_1$ was used as references because it was independent of local ligand field and the value of A_{01} was estimated to be ≈50 s^{-1} and A_{0J} was obtained by using the following relation in equation (2) [40, 41]:

$$A_{0J} = A_{01}\frac{I_{0J}\upsilon_{01}}{I_{01}\upsilon_{0J}} \tag{2}$$

Where I_{01} and I_{0J} are the integrated intensities of $^5D_0 \rightarrow {}^7F_1$ and $^5D_0 \rightarrow {}^7F_J$ transition (J = 2 and 4) and the energy barycenteres of these transitions are expressed by υ_{01} and υ_{oJ} respectively. The reciprocal of life time is the total decay rate which was determined from the calculated A_{rad} rates and the experimental decay rates by following equation (3) [42]:

$$\frac{1}{\tau} = A_{rad}+A_{nrad} \tag{3}$$

From Table 3 it can be concluded that the complex 1 exhibited the lowest luminescent quantum efficiency (14.94) due to presence of two water molecules in the coordination sphere of complex. The O-H oscillator effectively quenches the luminescence of the Eu^{3+} ion. On the other hand, complexes 2–6 exhibited high quantum efficiency as the ancillary ligand displaced the water molecules from the coordination sphere of the complexes, thereby making an efficient energy transfer from ligands to emitting center [1]. The complexes 3–6 exhibited better quantum efficiency than that of complex 2 because of the presence of additional aromatic chromophore moieties in the ancillary ligand 3–6 which can be improve the radiative properties of the Eu^{3+} complexes. Moreover, complex 6 exhibited highest quantum efficiency due to extended conjugation induced by two phenyl rings in the 4,7-positions of the bathophenanthroline [38].

Judd-Ofelt Intensity Parameters

The Judd-Ofelt intensity parameter (J-O) is very useful to tell about the possible chemical environment around the europium ion. In the standard Judd-Ofelt theory of 4f-4f intensities, Ω_t intensity parameters contain the contributions from the forced electric dipole and dynamic coupling mechanisms [43]. According to J-O theory, electronic transition state $^5D_0 \rightarrow {}^7F_J$ levels with J = 0, 3 or 5 are electrically as well as magnificently forbidden [44]. Therefore, in order to examine

Table 3 Photoluminescence data of Eu(III) complexes 1–6 in solid state

Complexes	τ (ms)	$A_{tot}(s^{-1})$	$A_{rad}(s^{-1})$	$A_{nrad}(s^{-1})$	Ω_2 (10^{-20} cm^2)	Ω_4 (10^{-20} cm^2)	η(%)
1	0.493	2331.58	303.19	2028.39	9.98	0.26	14.94
2	0.632	1916.81	334.54	1582.27	11.04	0.21	21.14
3	0.842	1527.62	339.98	1187.64	11.21	0.24	28.62
4	0.867	1496.04	342.64	1153.40	11.29	0.26	29.70
5	0.896	1471.59	355.52	1116.07	11.73	0.23	31.85
6	0.912	1468.31	371.82	1096.49	11.78	0.89	34.43

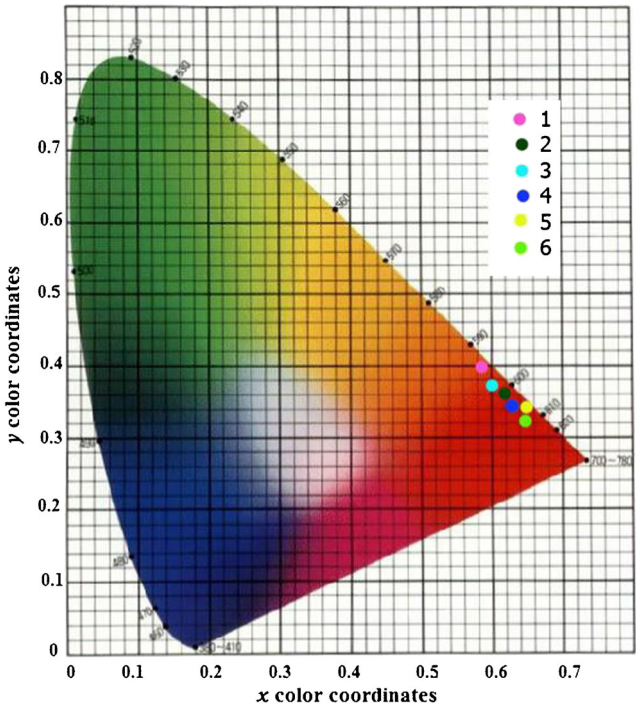

Fig. 4 CIE coordinate diagram of Eu(III) complexes 1–6

the possible structural changes around the Eu^{3+} ion, the intensities parameters Ω_2 and Ω_4 were calculated from the emission spectra (Fig. 2) using the $^5D_0 \rightarrow {}^7F_2$ and $^5D_0 \rightarrow {}^7F_4$ as per equation [45]:

$$\Omega_t = \frac{3\hbar c^3 A_{oJ}}{4e^2\omega^3\chi\left\langle {}^5D_0 \| U^{(t)} \| {}^7F_J \right\rangle^2} \quad (4)$$

Where Ω is the angular frequency of the transition, $\chi = n_0^2\left(n_0^2+2\right)^2/9$ is a Lorentz local field correction and an average index of refraction equal to 1.5 was used. The squared reduced matrix element is independent of the chemical environment of the Eu^{3+} ion and is 0.0032 for $\langle {}^5D_0 \| U^{(2)} \| {}^7F_2\rangle^2$ and 0.0023 for $\langle {}^5D_0 \| U^{(4)} \| {}^7F_4\rangle^2$. The experimental value of J-O intensities parameters Ω_2 and Ω_4 are tabulated in Table 3, which reflect the local structure and bonding in the environment of Eu^{3+} ion. The value of Ω_2 parameter indicates the hypersensitive behaviour of the $^5D_0 \rightarrow {}^7F_2$ transition, which reflects that the Eu^{3+} ions are located in a higher polarisable chemical environment.

Antimicrobial Activity

The synthesized ligand CHME and its corresponding Eu(III) complexes 1–6 were evaluated for their in vitro antibacterial activity against Gram-positive bacteria: *S. aureus*, *B. subtilis* and Gram-negative bacterium: *E. coli* and fungal strains: *C. albicans* and *A. niger* using tube dilution method using ciprofloxacin (antibacterial) and fluconazole (antifungal) as reference standard drugs. The values of the MIC against

Table 4 Minimum inhibitory concentration of HDMPE and its corresponding Eu(III) complexes [1–6]

Compound	Minimum Inhibitory Concentration (μM/mL)				
	B. subtillis	*S.aureus*	*E.coli*	*C.albicans*	*A.niger*
CHME	22.5	22.5	22.5	45.2	45.2
bipy	1.99	1.99	1.99	1.99	1.99
neo	0.74	1.49	1.49	1.49	1.49
phen	1.73	0.86	1.73	1.73	1.73
dmphen	0.74	1.49	1.49	0.74	0.74
bathophen	0.46	0.93	0.93	0.46	0.46
1	12.3	6.15	6.15	12.4	6.15
2	11.0	5.50	5.50	11.0	5.50
3	10.5	5.25	5.25	10.5	5.50
4	10.7	5.39	5.39	10.7	5.39
5	10.5	5.25	5.25	10.5	5.50
6	9.50	4.75	4.75	9.50	4.75
Std.	8.71[a]	8.71[a]	8.71[a]	10.09[b]	10.09[b]

[a] Ciprofloxacin

[b] Fluconazole

microorganisms tested are presented in Table 4. The antibacterial activity results indicated that the synthesized ligand CHME was found to be inactive, whereas all the complexes showed more active than the standard drug against *S. aureus* and *E. coli* bacteria. In case of antifungal activity all the complexes exhibited excellent activity than the standard drug fluconazole against *A. niger*, whereas moderate activity showed by all the complexes against *C. albicans*.

Finally it can be concluded that all the complexes are potent antimicrobial agent due to increase π-conjugation present in the complexes. Moreover, it was interesting to note that all the complexes proved to be better than the standard references (ciprofloxacin and fluconazole) in case of the microbes *S. aureus, E. coli* and *A. niger.* This may be occurs due to the complexatation of trivalent europium ion with β-hydroxyketone ligand 2-(4-chlorophenyl)-1-(2-hydroxy-4-

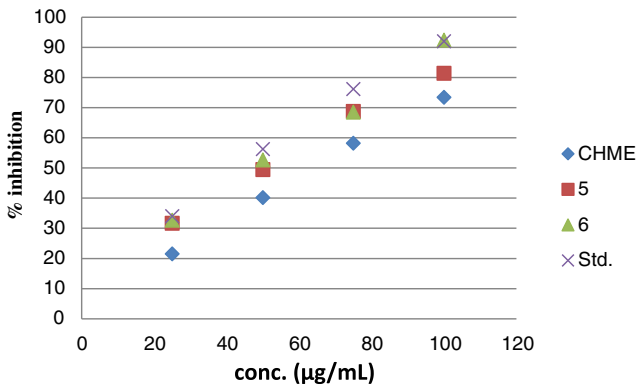

Fig. 5 Percentage inhibition values of CHME, Eu(III) complexes 5 and 6 with respect to standard ascorbic acid

Table 5 Percentage inhibition and IC_{50} values of DPPH radical scavenging activity of synthesized CHME and its corresponding Eu(III) complexes 1–6

Compound	Concentration (μg/mL)				
	25	50	75	100	IC_{50}
CHME	21.56	40.21	58.23	73.46	64.84
1	25.68	42.65	61.54	81.74	58.62
2	23.78	42.72	64.56	78.46	59.32
3	22.46	46.74	64.25	80.67	57.94
4	28.67	47.62	63.58	83.24	54.47
5	31.68	49.43	68.78	81.37	50.98
6	32.68	52.68	68.54	92.37	47.74
Std.	34.02	56.22	76.12	92.01	43.78

methoxyphenyl)ethan-1-one. In the complexes Eu(III) ion coordinated with the donor oxygen and nitrogen atoms of the ligand CHME and ancillary ligands respectively which leads to the π-electron delocalization over the chelate ring [46]. Furthermore, it was noticed that the antimicrobial activity of the synthesized complexes increases with the increasing π-conjugation system present in the complexes.

In Vitro Antioxidant Activity

The nitrogen centered stable free radical DPPH has been broadly used in spectrophotometer to characterize antioxidants [47]. The DPPH scavenging activity is expressed as IC_{50}. The IC_{50} values were calculated from the graph plotted as inhibition percentage against concentration of ligand CHME and complexes as shown in Fig. 5. The observed data of antioxidant activity of synthesized ligand CHME and its Eu(III) complexes 1–6 were tabulated in Table 5. The results revealed that The ligand CHME (IC_{50} = 64.84 μg/mL) showed poor activity, whereas all the synthesized complexes exhibited significant antioxidant activity, with the strongest being observed in complex $Eu(CHME)_3$.bathophen (IC_{50} = 47.74 μg/mL) when compared with the standard ascorbic acid (IC_{50} = 43.78 μg/mL).

Conclusion

This work reports the synthesis of a series of six novel Eu(III) complexes, $Eu(CHME)_3.2H_2O$ [1] $Eu(CHME)_3$.bipy [2], $Eu(CHME)_3$.neo [3], $Eu(CHME)_3$.phen [4], $Eu(CHME)_3$.dmphen [5] and $Eu(CHME)_3$.bathophen [6] by employing CHME as main ligand and bipy or neo or phen or dmphen or bathophen as ancillary ligand. Compositions of these complexes have been confirmed by elemental analysis, FT-IR, ^{1}H-NMR and ^{13}C-NMR. The photoluminescence properties such as excitation spectra, emission spectra as well as decay curves have also been investigated in solid state. The emission spectra of all the complexes exhibited four characteristic transitions assigned to $^5D_0 \rightarrow {}^7F_1$ (593 nm), $^5D_0 \rightarrow {}^7F_2$ (617 nm), $^5D_0 \rightarrow {}^7F_3$ (650 nm) and $^5D_0 \rightarrow {}^7F_4$ (684 nm). The $^5D_0 \rightarrow {}^7F_2$ transition is approximately 3–6 times stronger than $^5D_0 \rightarrow {}^7F_1$ transition, indicating a highly polarisable chemical environment around the central Eu^{3+} ion responsible for the bright red color of these complexes. These complexes might be promising photoluminescent materials for the fabrication of display devices. The photoluminescence analysis of the radiative decay rate A_{rad}, nonradiative rates A_{nrad}, the lifetime values (τ) and the luminescence quantum yield (η) confirmed that ancillary ligands could enhanced the photoluminescence properties of the Eu(III) complexes with the β-hydroxyketone 2-(4-chlorophenyl)-1-(2-hydroxy-4-methoxyphenyl)ethan-1-one. Moreover, it was interesting to note that all the complexes proved to be having better antimicrobial activity than the standard references (ciprofloxacin and fluconazole) in case of the microbes *S. aureus, E. coli* and *C. albicans.*

References

1. Yang C, Luo J, Ma J, Lu M, Liang L, Tong B (2011) Dyes Pigments 92:696
2. C. Adachi, M.A. Baldo, S.R. Forrest (2000) J Appl Phys 87: 8049.
3. Quirino WG, Legnani C, Dos Santos R, Teixeira K, Cremona M, Guedes M, Brito HF (2008) Thin Solid Films:517–1096
4. J.Kido, Okamoto Y (2002) Chem Rev 102:2357
5. Takada N, Tsutsui T, Saito S (1994) Jpn J Appl Phys 33:863
6. Kido J, Nagai K, Okamoto Y (1993) J Alloys Compd 192:30
7. Cristiano R, Westphal E, Bechtold IH, Bortoluzzi AJ, Gallardo H (2007) Tetrahedron 63:2851
8. Klink SI, Grave L, Reinhoudt DN, Van Veggel FCJM, Wertz MHV, Geurtz FAJ, Hofstraat JW (2000) J Phys Chem A
9. I. Hemmila (1995) J Alloys Compd 225: 480.
10. Moynagh J, Schimmel H (1999) Nature 400:105
11. Lenaerts P, Driesen K, Van Deun R, Binnemans K (2005) Chem Mater 17(8):2148
12. Schaferling M, Wolfbeis OS (2007) Chem-Eur J 13(15):4342
13. Aarons RJ, Notta JK, Meloni MM, Feng J, Vidyasager R, Narvainen J, Lian S, Spencer N, Kauppinen RA, Snaith JS, Faulkner S (2006) Chem Commun (8):909
14. J.C.G. Bunzli, S. Comby, A.S. Chauvin, C.D.B. Vandevyver (2007) J Rare Earths 25: 257.
15. Cui Y, Yue Y, Qian G, Chen B (2012) Chem Rev 112:1126
16. E. G. Moore, A.P.S. Samuel, K.N. Raymond (2009) Acc ChemRes 42: 542.
17. Chen FF, Chen ZQ, Bian ZQ, Huang CH (2010) Coord Chem Rev 254:991
18. S.P. Sinha, Complexes of Rare Earths (1996) Pergamon Press, UK 134.
19. Wang J, Yang ZY, Wang BD, Yi XY, Liu YC (2009) J Fluoresc 19: 847
20. Liu JY, Ren N, Zheng JJ, Zhang CY (2013) Thermochim Acta 570: 5
21. Yang Y, Zhang SY (2004) Spectrochim. Acta Part A 60:2065

22. Liang TYR, Zhao Y, Song Y, Gao B, Li M, Min L, Zhang H, Fan D (2015) Ployhedron 85:789
23. Wertz MHV, Duin MA, Hofstraat JW, Verhoeven JW (1999) Chem Commun:799
24. Gawryszewska P, Jerzykiewicz L, Pietraszkiewicz M, Legendziewicz J, Riehl JP (2000) Inorg Chem 39:5365
25. Jiang X, Wu Y, He C (2008) Mater Lett 62:286
26. Luo Y-M, Chen Z, Tang R-R, Xiao L-X, Peng H-J (2008) Spectrochim Acta Part A 69:513
27. J. Bao, Z. Zhang, R. Tang, H. Han, Z. Yang (2013) J Lumin 136: 68.
28. Percy GC (1976) Spectrochim Acta A 32:1287
29. Tian L, Ren N, Zhang JJ, Sun SJ, Ye HM, Bai JH, Wang RF (2009) J Chem Eng Data 54(1):69
30. Z.A. Taha, A. M. Ajlouni, A.K. Hijazi, N.A. A-Rawashdeh, K.A. Al-Hassan, Y.A. Al-Haj, M.A. Ebqaai, A.Y. Altalafha (2015) J Lumin 161: 229.
31. G. Zucchi, V. Murugesan, D. Tondelier, D. Aldakov, T. Jeon, F. Yang, P. Thuery, M. Ephiritikhine, B. Geffroy (2011) Inorg Chem 50: 4851.
32. Wang YB, Zheng XJ, Zhuang WJ, Jin LP (2003) Eur J Inorg Chem: 1355
33. Li H-F, Yan P-F, Yan PC, Xu WH, Li G–M (2012) Dalton Trans 41:900
34. Binnemans K (2009) Chem Rev 109:4283
35. Xu J, Zhang Y, Chen H, Liu WS, Tang Y (2014) Daltons 43:7903
36. Shi PF, Cheng P, Zhao B (2012) Cryst Growth Des 12:5203
37. Y.S. Zhou, Y. Guo, S. Xu, L.J. Zhang (2013) Inorg Chem 52: 6338.
38. Ambili Raj DB, Biju S, Reddy MLP (2008) Inorg Chem 47:8091
39. Wertz MHV, Jukes RTF, Verhoeven JW (2002) Phys Chem Chem Phys 4:1542
40. Carlos LD, Messaddeq Y, Brito HF, Ferreira RAS, Bermudez VD, Ribeiro SJL (2000) Adv Mater 12:594
41. Wang D, Zheng C, Fan L, Hu Y, Zheng J (2014) Spectrochim Acta Part A 117:245
42. Donega Cd M, Alves S Jr, Sa GFd (1997) J Alloys Compd 250:422
43. Binnemans K, Hreck KV, Walrand CG (1997) Chem Phys Lett 266: 297
44. Ofelt GS (1962) J Chem Phys 37:511
45. Teotonio EES, Brito HF, Felinto MCFC, Kodaira CA, Malta OL (2003) J Coord Chem 56:913
46. Liu JY, Ren N, Zhang JJ, Zhang CY (2013) Thermochim Acta 570:51
47. Doan TN, Tran DT (2011) Pharmacology & Pharmacy 2:282